

Cold-Nuclear-Matter Effects on Heavy-Quark Production at Forward and Backward Rapidity in $d + \text{Au}$ Collisions at $\sqrt{s_{NN}} = 200 \text{ GeV}$

- A. Adare,¹³ C. Aidala,^{38,42,43} N. N. Ajitanand,⁶⁰ Y. Akiba,^{55,56} R. Akimoto,¹² H. Al-Bataineh,⁴⁹ H. Al-Ta'ani,⁴⁹ J. Alexander,⁶⁰ K. R. Andrews,¹ A. Angerami,¹⁴ K. Aoki,^{34,55} N. Apadula,⁶¹ E. Appelt,⁶⁵ Y. Aramaki,^{12,55} R. Armendariz,⁸ E. C. Aschenauer,⁷ E. T. Atomssa,³⁵ R. Averbeck,⁶¹ T. C. Awes,⁵¹ B. Azmoun,⁷ V. Babintsev,²⁴ M. Bai,⁶ G. Baksay,¹⁹ L. Baksay,¹⁹ B. Bannier,⁶¹ K. N. Barish,⁸ B. Bassalleck,⁴⁸ A. T. Basye,¹ S. Bathe,^{5,8,56} V. Baublis,⁵⁴ C. Baumann,⁴⁴ A. Bazilevsky,⁷ S. Belikov,^{7,*} R. Belmont,⁶⁵ J. Ben-Benjamin,⁴⁵ R. Bennett,⁶¹ J. H. Bhom,⁶⁹ D. S. Blau,³³ J. S. Bok,⁶⁹ K. Boyle,^{56,61} M. L. Brooks,³⁸ D. Broxmeyer,⁴⁵ H. Buesching,⁷ V. Bumazhnov,²⁴ G. Bunce,^{7,56} S. Butsyk,³⁸ S. Campbell,⁶¹ A. Caringi,⁴⁵ P. Castera,⁶¹ C.-H. Chen,⁶¹ C. Y. Chi,¹⁴ M. Chiu,⁷ I. J. Choi,^{25,69} J. B. Choi,¹⁰ R. K. Choudhury,⁴ P. Christiansen,⁴⁰ T. Chujo,⁶⁴ P. Chung,⁶⁰ O. Chvala,⁸ V. Cianciolo,⁵¹ Z. Citron,⁶¹ B. A. Cole,¹⁴ Z. Conesa del Valle,³⁵ M. Connors,⁶¹ M. Csand,¹⁷ T. Csorgo,⁶⁸ T. Dahms,⁶¹ S. Dairaku,^{34,55} I. Danchev,⁶⁵ K. Das,²⁰ A. Datta,⁴² G. David,⁷ M. K. Dayananda,²¹ A. Denisov,²⁴ A. Deshpande,^{56,61} E. J. Desmond,⁷ K. V. Dharmawardane,⁴⁹ O. Dietzsch,⁵⁸ A. Dion,^{28,61} M. Donadelli,⁵⁸ O. Drapier,³⁵ A. Drees,⁶¹ K. A. Drees,⁶ J. M. Durham,^{38,61} A. Durum,²⁴ D. Dutta,⁴ L. D'Orazio,⁴¹ S. Edwards,²⁰ Y. V. Efremenko,⁵¹ F. Ellinghaus,¹³ T. Engelmore,¹⁴ A. Enokizono,⁵¹ H. En'yo,^{55,56} S. Esumi,⁶⁴ B. Fadem,⁴⁵ D. E. Fields,⁴⁸ M. Finger,⁹ M. Finger, Jr.,⁹ F. Fleuret,³⁵ S. L. Fokin,³³ Z. Fraenkel,^{67,*} J. E. Frantz,^{50,61} A. Franz,⁷ A. D. Frawley,²⁰ K. Fujiwara,⁵⁵ Y. Fukao,⁵⁵ T. Fusayasu,⁴⁷ C. Gal,⁶¹ I. Garishvili,⁶² A. Glenn,³⁷ H. Gong,⁶¹ X. Gong,⁶⁰ M. Gonin,³⁵ Y. Goto,^{55,56} R. Granier de Cassagnac,³⁵ N. Grau,^{2,14} S. V. Greene,⁶⁵ G. Grim,³⁸ M. Grosse Perdekamp,²⁵ T. Gunji,¹² L. Guo,³⁸ H.-Å. Gustafsson,^{40,*} J. S. Haggerty,⁷ K. I. Hahn,¹⁸ H. Hamagaki,¹² J. Hamblen,⁶² R. Han,⁵³ J. Hanks,¹⁴ C. Harper,⁴⁵ K. Hashimoto,^{55,57} E. Haslum,⁴⁰ R. Hayano,¹² X. He,²¹ M. Heffner,³⁷ T. K. Hemmick,⁶¹ T. Hester,⁸ J. C. Hill,²⁸ M. Hohlmann,¹⁹ R. S. Hollis,⁸ W. Holzmann,¹⁴ K. Homma,²³ B. Hong,³² T. Horaguchi,^{23,64} Y. Hori,¹² D. Hornback,^{51,62} S. Huang,⁶⁵ T. Ichihara,^{55,56} R. Ichimiya,⁵⁵ H. Iinuma,³¹ Y. Ikeda,⁶⁴ K. Imai,^{29,34,55} M. Inaba,⁶⁴ A. Iordanova,⁸ D. Isenhower,¹ M. Ishihara,⁵⁵ M. Issah,⁶⁵ D. Ivanischev,⁵⁴ Y. Iwanaga,²³ B. V. Jacak,⁶¹ J. Jia,^{7,60} X. Jiang,³⁸ J. Jin,¹⁴ D. John,⁶² B. M. Johnson,⁷ T. Jones,¹ K. S. Joo,⁴⁶ D. Jouan,⁵² D. S. Jumper,¹ F. Kajihara,¹² J. Kamin,⁶¹ S. Kaneti,⁶¹ B. H. Kang,²² J. H. Kang,²² J. Kapustinsky,³⁸ K. Karatsu,^{34,55} M. Kasai,^{55,57} D. Kawall,^{42,56} M. Kawashima,^{55,57} A. V. Kazantsev,³³ T. Kempel,²⁸ A. Khanzadeev,⁵⁴ K. M. Kijima,²³ J. Kikuchi,⁶⁶ A. Kim,¹⁸ B. I. Kim,³² D. J. Kim,³⁰ E.-J. Kim,¹⁰ Y.-J. Kim,²⁵ Y. K. Kim,²² E. Kinney,¹³ A. Kiss,¹⁷ E. Kistenev,⁷ D. Kleijnjan,⁸ P. Kline,⁶¹ L. Kochenda,⁵⁴ B. Komkov,⁵⁴ M. Konno,⁶⁴ J. Koster,²⁵ D. Kotov,⁵⁴ A. Krl,¹⁵ A. Kravitz,¹⁴ G. J. Kunde,³⁸ K. Kurita,^{55,57} M. Kurosawa,⁵⁵ Y. Kwon,⁶⁹ G. S. Kyle,⁴⁹ R. Lacey,⁶⁰ Y. S. Lai,¹⁴ J. G. Lajoie,²⁸ A. Lebedev,²⁸ D. M. Lee,³⁸ J. Lee,¹⁸ K. B. Lee,³² K. S. Lee,³² S. H. Lee,⁶¹ S. R. Lee,¹⁰ M. J. Leitch,³⁸ M. A. L. Leite,⁵⁸ X. Li,¹¹ P. Lichtenwalner,⁴⁵ P. Liebing,⁵⁶ S. H. Lim,⁶⁹ L. A. Linden Levy,¹³ T. Lika,¹⁵ H. Liu,³⁸ M. X. Liu,³⁸ B. Love,⁶⁵ D. Lynch,⁷ C. F. Maguire,⁶⁵ Y. I. Makdisi,⁶ M. D. Malik,⁴⁸ A. Manion,⁶¹ V. I. Manko,³³ E. Mannel,¹⁴ Y. Mao,^{53,55} H. Masui,⁶⁴ F. Matathias,¹⁴ M. McCumber,^{13,61} P. L. McGaughey,³⁸ D. McGlinchey,^{13,20} C. McKinney,²⁵ N. Means,⁶¹ M. Mendoza,⁸ B. Meredith,²⁵ Y. Miake,⁶⁴ T. Mibe,³¹ A. C. Mignerey,⁴¹ K. Miki,^{55,64} A. Milov,^{7,67} J. T. Mitchell,⁷ Y. Miyachi,^{55,63} A. K. Mohanty,⁴ H. J. Moon,⁴⁶ Y. Morino,¹² A. Morreale,⁸ D. P. Morrison,^{7,†} S. Motschwiller,⁴⁵ T. V. Moukhanova,³³ T. Murakami,³⁴ J. Murata,^{55,57} S. Nagamiya,³¹ J. L. Nagle,^{13,‡} M. Naglis,⁶⁷ M. I. Nagy,⁶⁸ I. Nakagawa,^{55,56} Y. Nakamiya,²³ K. R. Nakamura,^{34,55} T. Nakamura,⁵⁵ K. Nakano,⁵⁵ S. Nam,¹⁸ J. Newby,³⁷ M. Nguyen,⁶¹ M. Nihashi,²³ R. Nouicer,⁷ A. S. Nyanin,³³ C. Oakley,²¹ E. O'Brien,⁷ S. X. Oda,¹² C. A. Ogilvie,²⁸ M. Oka,⁶⁴ K. Okada,⁵⁶ Y. Onuki,⁵⁵ A. Oskarsson,⁴⁰ M. Ouchida,^{23,55} K. Ozawa,¹² R. Pak,⁷ V. Pantuev,^{26,61} V. Papavassiliou,⁴⁹ B. H. Park,²² I. H. Park,¹⁸ S. K. Park,³² W. J. Park,³² S. F. Pate,⁴⁹ L. Patel,²¹ H. Pei,²⁸ J.-C. Peng,²⁵ H. Pereira,¹⁶ D. Yu. Peressounko,³³ R. Petti,⁶¹ C. Pinkenburg,⁷ R. P. Pisani,⁷ M. Proissl,⁶¹ M. L. Purschke,⁷ H. Qu,²¹ J. Rak,³⁰ I. Ravinovich,⁶⁷ K. F. Read,^{51,62} S. Rembeczki,¹⁹ K. Reygers,⁴⁴ V. Riabov,⁵⁴ Y. Riabov,⁵⁴ E. Richardson,⁴¹ D. Roach,⁶⁵ G. Roche,³⁹ S. D. Rolnick,⁸ M. Rosati,²⁸ C. A. Rosen,¹³ S. S. E. Rosendahl,⁴⁰ P. Ruika,²⁷ B. Sahlmueller,^{44,61} N. Saito,³¹ T. Sakaguchi,⁷ K. Sakashita,^{55,63} V. Samsonov,⁵⁴ S. Sano,^{12,66} M. Sarsour,²¹ T. Sato,⁶⁴ M. Savastio,⁶¹ S. Sawada,³¹ K. Sedgwick,⁸ J. Seele,¹³ R. Seidl,^{25,56} R. Seto,⁸ D. Sharma,⁶⁷ I. Shein,²⁴ T.-A. Shibata,^{55,63} K. Shigaki,²³ H. H. Shim,³² M. Shimomura,⁶⁴ K. Shoji,^{34,55} P. Shukla,⁴ A. Sickles,⁷ C. L. Silva,²⁸ D. Silvermyr,⁵¹ C. Silvestre,¹⁶ K. S. Sim,³² B. K. Singh,³ C. P. Singh,³ V. Singh,³ M. Slunecka,⁹ T. Sodre,⁴⁵ R. A. Soltz,³⁷ W. E. Sondheim,³⁸ S. P. Sorensen,⁶² I. V. Sourikova,⁷ P. W. Stankus,⁵¹ E. Stenlund,⁴⁰ S. P. Stoll,⁷ T. Sugitate,²³ A. Sukhanov,⁷ J. Sun,⁶¹ J. Sziklai,⁶⁸ E. M. Takagui,⁵⁸ A. Takahara,¹² A. Taketani,^{55,56} R. Tanabe,⁶⁴ Y. Tanaka,⁴⁷ S. Taneja,⁶¹ K. Tanida,^{34,55,56,59} M. J. Tannenbaum,⁷ S. Tarafdar,³ A. Taranenko,⁶⁰ E. Tennant,⁴⁹ H. Themann,⁶¹ D. Thomas,¹ T. L. Thomas,⁴⁸ M. Togawa,⁵⁶ A. Toia,⁶¹ L. Tomasek,²⁷ M. Tomasek,²⁷ H. Torii,²³ R. S. Towell,¹ I. Tserruya,⁶⁷ Y. Tsuchimoto,²³ K. Utsunomiya,¹²

C. Vale,⁷ H. Valle,⁶⁵ H. W. van Hecke,³⁸ E. Vazquez-Zambrano,¹⁴ A. Veicht,^{14,25} J. Velkovska,⁶⁵ R. Vértesi,⁶⁸ M. Virius,¹⁵ A. Vossen,²⁵ V. Vrba,²⁷ E. Vznuzdaev,⁵⁴ X. R. Wang,⁴⁹ D. Watanabe,²³ K. Watanabe,⁶⁴ Y. Watanabe,^{55,56} Y. S. Watanabe,¹² F. Wei,²⁸ R. Wei,⁶⁰ J. Wessels,⁴⁴ S. N. White,⁷ D. Winter,¹⁴ C. L. Woody,⁷ R. M. Wright,¹ M. Wysocki,¹³ Y. L. Yamaguchi,^{12,55} K. Yamaura,²³ R. Yang,²⁵ A. Yanovich,²⁴ J. Ying,²¹ S. Yokkaichi,^{55,56} J. S. Yoo,¹⁸ Z. You,^{38,53} G. R. Young,⁵¹ I. Younus,^{36,48} I. E. Yushmanov,³³ W. A. Zajc,¹⁴ A. Zelenski,⁶ and S. Zhou¹¹

(PHENIX Collaboration)

¹Abilene Christian University, Abilene, Texas 79699, USA

²Department of Physics, Augustana College, Sioux Falls, South Dakota 57197, USA

³Department of Physics, Banaras Hindu University, Varanasi 221005, India

⁴Bhabha Atomic Research Centre, Bombay 400 085, India

⁵Baruch College, City University of New York, New York, New York 10010, USA

⁶Collider-Accelerator Department, Brookhaven National Laboratory, Upton, New York 11973-5000, USA

⁷Physics Department, Brookhaven National Laboratory, Upton, New York 11973-5000, USA

⁸University of California-Riverside, Riverside, California 92521, USA

⁹Charles University, Ovocný trh 5, Praha 1, 116 36, Prague, Czech Republic

¹⁰Chonbuk National University, Jeonju, 561-756, Korea

¹¹Science and Technology on Nuclear Data Laboratory, China Institute of Atomic Energy, Beijing 102413, People's Republic of China

¹²Center for Nuclear Study, Graduate School of Science, University of Tokyo, 7-3-1 Hongo, Bunkyo, Tokyo 113-0033, Japan

¹³University of Colorado, Boulder, Colorado 80309, USA

¹⁴Columbia University, New York, New York 10027 and Nevis Laboratories, Irvington, New York 10533, USA

¹⁵Czech Technical University, Zikova 4, 166 36 Prague 6, Czech Republic

¹⁶Dapnia, CEA Saclay, F-91191, Gif-sur-Yvette, France

¹⁷ELTE, Eötvös Loránd University, H-1117 Budapest, Pázmány P. s. 1/A, Hungary

¹⁸Ewha Womans University, Seoul 120-750, Korea

¹⁹Florida Institute of Technology, Melbourne, Florida 32901, USA

²⁰Florida State University, Tallahassee, Florida 32306, USA

²¹Georgia State University, Atlanta, Georgia 30303, USA

²²Hanyang University, Seoul 133-792, Korea

²³Hiroshima University, Kagamiyama, Higashi-Hiroshima 739-8526, Japan

²⁴IHEP Protvino, State Research Center of Russian Federation, Institute for High Energy Physics, Protvino 142281, Russia

²⁵University of Illinois at Urbana-Champaign, Urbana, Illinois 61801, USA

²⁶Institute for Nuclear Research of the Russian Academy of Sciences, prospekt 60-letiya Oktyabrya 7a, Moscow 117312, Russia

²⁷Institute of Physics, Academy of Sciences of the Czech Republic, Na Slovance 2, 182 21 Prague 8, Czech Republic

²⁸Iowa State University, Ames, Iowa 50011, USA

²⁹Advanced Science Research Center, Japan Atomic Energy Agency, 2-4 Shirakata Shirane, Tokai-mura, Naka-gun, Ibaraki-ken 319-1195, Japan

³⁰Helsinki Institute of Physics and University of Jyväskylä, P.O.Box 35, FI-40014 Jyväskylä, Finland

³¹KEK, High Energy Accelerator Research Organization, Tsukuba, Ibaraki 305-0801, Japan

³²Korea University, Seoul 136-701, Korea

³³Russian Research Center "Kurchatov Institute", Moscow 123098, Russia

³⁴Kyoto University, Kyoto 606-8502, Japan

³⁵Laboratoire Leprince-Ringuet, Ecole Polytechnique, CNRS-IN2P3, Route de Saclay, F-91128 Palaiseau, France

³⁶Physics Department, Lahore University of Management Sciences, Lahore 54792, Pakistan

³⁷Lawrence Livermore National Laboratory, Livermore, California 94550, USA

³⁸Los Alamos National Laboratory, Los Alamos, New Mexico 87545, USA

³⁹LPC, Université Blaise Pascal, CNRS-IN2P3, Clermont-Fd, 63177 Aubiere Cedex, France

⁴⁰Department of Physics, Lund University, Box 118, SE-221 00 Lund, Sweden

⁴¹University of Maryland, College Park, Maryland 20742, USA

⁴²Department of Physics, University of Massachusetts, Amherst, Massachusetts 01003-9337, USA

⁴³Department of Physics, University of Michigan, Ann Arbor, Michigan 48109-1040, USA

⁴⁴Institut für Kernphysik, University of Muenster, D-48149 Muenster, Germany

⁴⁵Muhlenberg College, Allentown, Pennsylvania 18104-5586, USA

⁴⁶Myongji University, Yongin, Kyonggido 449-728, Korea

⁴⁷Nagasaki Institute of Applied Science, Nagasaki-shi, Nagasaki 851-0193, Japan

⁴⁸University of New Mexico, Albuquerque, New Mexico 87131, USA

⁴⁹New Mexico State University, Las Cruces, New Mexico 88003, USA

⁵⁰Department of Physics and Astronomy, Ohio University, Athens, Ohio 45701, USA

⁵¹*Oak Ridge National Laboratory, Oak Ridge, Tennessee 37831, USA*⁵²*IPN-Orsay, Université Paris Sud, CNRS-IN2P3, BPI, F-91406 Orsay, France*⁵³*Peking University, Beijing 100871, People's Republic of China*⁵⁴*PNPI, Petersburg Nuclear Physics Institute, Gatchina, Leningrad Region 188300, Russia*⁵⁵*RIKEN Nishina Center for Accelerator-Based Science, Wako, Saitama 351-0198, Japan*⁵⁶*RIKEN BNL Research Center, Brookhaven National Laboratory, Upton, New York 11973-5000, USA*⁵⁷*Physics Department, Rikkyo University, 3-34-1 Nishi-Ikebukuro, Toshima, Tokyo 171-8501, Japan*⁵⁸*Universidade de São Paulo, Instituto de Física, Caixa Postal 66318, São Paulo CEP05315-970, Brazil*⁵⁹*Seoul National University, Seoul, Korea*⁶⁰*Chemistry Department, Stony Brook University, SUNY, Stony Brook, New York 11794-3400, USA*⁶¹*Department of Physics and Astronomy, Stony Brook University, SUNY, Stony Brook, New York 11794-3400, USA*⁶²*University of Tennessee, Knoxville, Tennessee 37996, USA*⁶³*Department of Physics, Tokyo Institute of Technology, Oh-okayama, Meguro, Tokyo 152-8551, Japan*⁶⁴*Institute of Physics, University of Tsukuba, Tsukuba, Ibaraki 305, Japan*⁶⁵*Vanderbilt University, Nashville, Tennessee 37235, USA*⁶⁶*Waseda University, Advanced Research Institute for Science and Engineering, 17 Kikui-cho, Shinjuku-ku, Tokyo 162-0044, Japan*⁶⁷*Weizmann Institute, Rehovot 76100, Israel*⁶⁸*Institute for Particle and Nuclear Physics, Wigner Research Centre for Physics, Hungarian Academy of Sciences**(Wigner RCP, RMKI) H-1525 Budapest 114, P.O. Box 49, Budapest, Hungary*⁶⁹*Yonsei University, IPAP, Seoul 120-749, Korea*

(Received 3 October 2013; revised manuscript received 24 January 2014; published 25 June 2014)

The PHENIX experiment has measured open heavy-flavor production via semileptonic decay over the transverse momentum range $1 < p_T < 6 \text{ GeV}/c$ at forward and backward rapidity ($1.4 < |y| < 2.0$) in $d + \text{Au}$ and $p + p$ collisions at $\sqrt{s_{NN}} = 200 \text{ GeV}$. In central $d + \text{Au}$ collisions, relative to the yield in $p + p$ collisions scaled by the number of binary nucleon-nucleon collisions, a suppression is observed at forward rapidity (in the d -going direction) and an enhancement at backward rapidity (in the Au-going direction). Predictions using nuclear-modified-parton-distribution functions, even with additional nuclear- p_T broadening, cannot simultaneously reproduce the data at both rapidity ranges, which implies that these models are incomplete and suggests the possible importance of final-state interactions in the asymmetric $d + \text{Au}$ collision system. These results can be used to probe cold-nuclear-matter effects, which may significantly affect heavy-quark production, in addition to helping constrain the magnitude of charmonia-breakup effects in nuclear matter.

DOI: 10.1103/PhysRevLett.112.252301

PACS numbers: 25.75.Dw

Heavy quarks are essential probes of the evolution of the medium created in heavy-ion collisions, because they are produced in the early stages of nuclear collisions. Heavy-quark production has been studied via semileptonic-decay electrons and muons, as well as fully reconstructed D mesons, at the Relativistic Heavy Ion Collider (RHIC) and the Large Hadron Collider [1,2]. In $p + p$ collisions, heavy-quark production tests perturbative quantum chromodynamics and provides a baseline for the results from heavy-ion collisions [3–5]. In central $\text{Au} + \text{Au}$ collisions at $\sqrt{s_{NN}} = 200 \text{ GeV}$, strong suppression of high-transverse-momentum (p_T) electrons from semileptonic decay of open heavy-flavor hadrons has been observed at midrapidity [6,7]. At forward rapidity, a similar level of suppression has been measured for the production of heavy-flavor muons in central $\text{Cu} + \text{Cu}$ collisions [8]. Although suppression of high- p_T particles was predicted as an effect of partonic energy loss in the dense medium created in heavy-ion collisions [9–11], the observed suppression is difficult to explain solely with hot-nuclear-matter effects [8,12]. To interpret such measurements, it is

essential to probe the underlying cold-nuclear-matter (CNM) effects, which may also be present.

Control experiments with $d + \text{Au}$ collisions allow us to probe those CNM effects, including modifications of the parton distribution functions (PDF) and nuclear- p_T broadening, with minimal impact from the hot nuclear medium. Because heavy quarks are produced primarily by gluon fusion at RHIC, modification of the gluon density in the nucleus can be observed in the charm and bottom production rates [13,14]. Based on PYTHIA [15] calculations, the average parton momentum fraction x in the Au nucleus leading to heavy-flavor muons with $1 < p_T^\mu < 6 \text{ GeV}/c$ at backward rapidity ($-2.0 < y < -1.4$, Au-going direction) and forward rapidity ($1.4 < y < 2.0$, d -going direction) is $\approx 8 \times 10^{-2}$ and $\approx 5 \times 10^{-3}$, respectively. Parton energy loss and multiple scattering in the nucleus can change the resulting heavy-flavor hadron momentum spectrum [16]. Previous results in $d + \text{Au}$ collisions at midrapidity show a significant enhancement of heavy-flavor electrons at moderate p_T [17]. In this Letter, we present measurements of the p_T spectra and the nuclear-modification factor (R_{dA}) of

negatively charged muons from open heavy flavor at forward and backward rapidity in $d + \text{Au}$ collisions at $\sqrt{s_{NN}} = 200$ GeV.

The $d + \text{Au}$ and $p + p$ data presented here were recorded with the PHENIX detector during the 2008 and 2009 RHIC running periods, respectively. Minimum-bias collisions are selected by using the beam-beam counter (BBC) [18], and this selection covers $88 \pm 4\%$ ($55 \pm 5\%$) of the total $d + \text{Au}$ ($p + p$) inelastic cross section [19]. The integrated luminosity, sampled using single muon triggers [8] in coincidence with the minimum-bias trigger, used for this analysis of $d + \text{Au}$ ($p + p$) collisions is 50 nb^{-1} (10 pb^{-1}). The $d + \text{Au}$ collisions are categorized into four centrality classes: 0%–20%, 20%–40%, 40%–60%, and 60%–88%, where 0%–20% represents the 20% highest multiplicity events, as determined by the amount of total charge deposited in the BBC on the Au-going side. For each centrality class, the average number of binary nucleon-nucleon collisions $\langle N_{\text{coll}} \rangle$ is calculated from the BBC charge in a Glauber model [20]. The values of $\langle N_{\text{coll}} \rangle$ for the $d + \text{Au}$ centrality classes specified above are 15.1 ± 1.0 , 10.2 ± 0.7 , 6.6 ± 0.4 , and 3.2 ± 0.2 , respectively. A correction for the underlying event correlation and the efficiency of the BBC trigger is applied, as in [21,22]. Unbiased collisions (0%–100%, $\langle N_{\text{coll}} \rangle = 7.6 \pm 0.4$) are also analyzed.

Two muon spectrometers [23] provide full azimuthal coverage in the pseudorapidity range $-2.2 < \eta < -1.2$ (backward rapidity) and $1.2 < \eta < 2.4$ (forward rapidity). Each muon arm, located behind copper (19 cm) and iron (60 cm) absorbers, comprises a muon tracker (MuTr) followed by a muon identifier (MuID). The MuTr comprises three stations of cathode strip chambers surrounded by a radial magnetic field, and the MuID comprises five interleaved layers of steel absorber and Iarocci tube planes. The MuTr provides the momentum measurement for charged tracks in the magnetic field. The momentum information for each charged track is then combined with its penetration depth reported by the MuID to provide effective discrimination between muons and hadrons (pion rejection rate: $\sim 10^{-3}$) [24].

Despite the large hadron rejection power of the muon arms and strict selection criteria, most of the tracks reaching the last MuID layer are not heavy-flavor muons. Simulation studies show that the majority of these background tracks for $p_T < 3 \text{ GeV}/c$ originate from the decays of light-flavor mesons (mostly π^\pm and K^\pm) into muons before reaching the absorber material. Another source of background, called “punch-through hadrons,” are the hadrons produced at the collision vertex, which penetrate all MuID layers. Other, less significant sources of background include muons from hadrons that decay inside the MuTr which are misreconstructed with erroneously high p_T , muons from heavy-flavor resonances (J/ψ , ψ' , and Υ), and muons from light vector mesons (ρ , ϕ , and ω). The J/ψ is the most

significant of these lesser sources, contributing less than 5% at high p_T [8,25]. The backgrounds are subtracted as follows.

For each data set, we measure the double differential heavy-flavor muon invariant yield, defined as

$$\frac{d^2N^\mu}{2\pi p_T dp_T dy} = \frac{1}{2\pi p_T \Delta p_T \Delta y} \frac{N_I - N_C - N_F - N_{J/\psi}}{(N_{\text{evt}}/\epsilon_{\text{BBC}})Ae}, \quad (1)$$

where Δp_T and Δy are the bin widths in p_T and y , N_I is the number of inclusive muon candidates, N_C is the number of decay and punch-through hadron background tracks determined using a hadron cocktail method (described below), N_F is the estimated number of fake tracks that pass the selection criteria, $N_{J/\psi}$ is the number of muons from J/ψ decays, N_{evt} is the number of sampled events, Ae is the detector acceptance and efficiency correction, and ϵ_{BBC} is the BBC bias-correction factor for the trigger efficiency and centrality determination of events containing a heavy-flavor muon. Only negative muons are used because the signal-to-background ratio is better than for positive muons [8]. The typical signal-to-background ratio, $N^\mu/(N_C + N_F + N_{J/\psi})$, increases from 0.3 at $p_T = 1 \text{ GeV}/c$ to 0.6 at $p_T = 6 \text{ GeV}/c$. The hadron-cocktail method estimates the overall background owing to light-hadron sources using a GEANT simulation based on measured p_T spectra. Details on the background-estimation procedure and associated systematic uncertainty are described in [3,8,25].

Figure 1 shows the invariant yield of heavy-flavor muons as a function of p_T in $d + \text{Au}$ collisions at backward and forward rapidity along with the invariant yield in $p + p$ collisions. The vertical bars represent statistical uncertainties, while boxes are systematic uncertainties in the acceptance and efficiency correction, background estimate, and trigger bias correction for each centrality class. The main source of the systematic uncertainty is the background estimate including initial hadron production ($\sim 10\%$) and interactions of hadrons with the absorber material ($\sim 10\%$). All components of the systematic uncertainty are added in quadrature. Solid lines show a modified Kaplan function $A(1 + [p_T/8.3(\text{GeV}/c)]^2)^{-3.9}$ [26], fit to the p_T spectrum in $p + p$ collisions, and then scaled by $\langle N_{\text{coll}} \rangle$ for each $d + \text{Au}$ centrality class. The $p + p$ results are consistent with previous PHENIX measurements [8].

To quantify nuclear effects in $d + \text{Au}$ collisions, we calculate the ratio of heavy-flavor muon yields in $d + \text{Au}$ to $p + p$ collisions scaled by the average number of binary collisions for a given centrality bin,

$$R_{dA} = \frac{dN_{dA}^{\mu^-}/dp_T}{\langle N_{\text{coll}} \rangle dN_{pp}^{\mu^-}/dp_T}. \quad (2)$$

Figure 2 shows R_{dA} as a function of p_T for heavy-flavor muons in different $d + \text{Au}$ centrality classes. Vertical bars

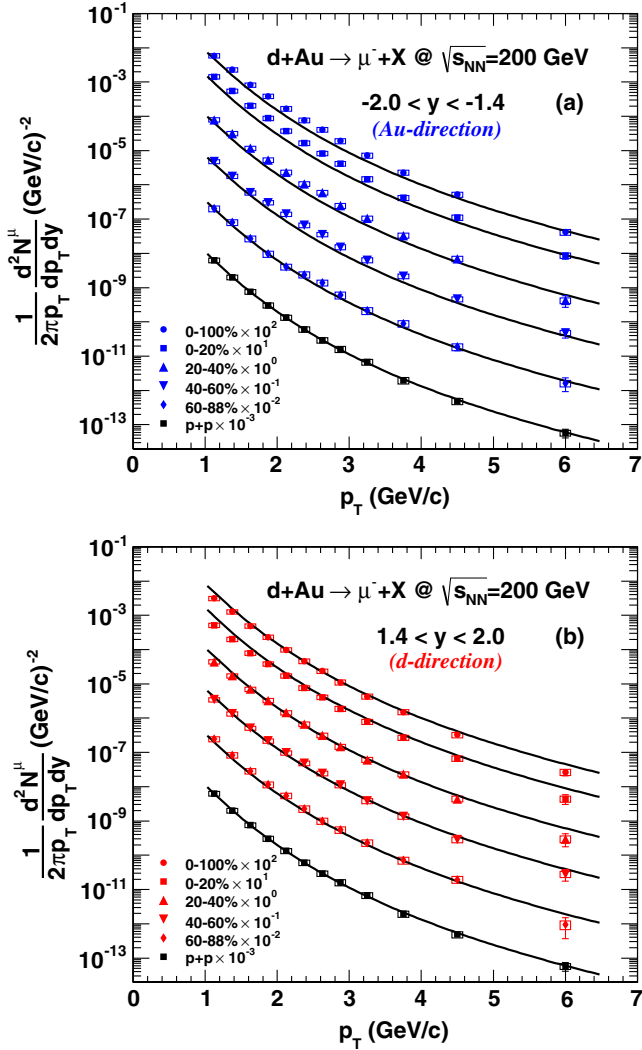


FIG. 1 (color online). Invariant yield of negatively charged heavy-flavor muons as a function of p_T in $p + p$ collisions at $\sqrt{s_{NN}} = 200$ GeV (black squares) and in $d + \text{Au}$ collisions for different centralities at (a) backward rapidity (Au-going) and (b) forward rapidity (d-going). The solid lines represent a fit to the $p + p$ invariant yield, scaled by the number of binary collisions $\langle N_{\text{coll}} \rangle$ for each centrality class.

(boxes) represent the statistical (systematic) uncertainties for R_{dA} , which are the quadratic sum of the uncertainties for the invariant yields of $p + p$ and $d + \text{Au}$ collisions. The systematic uncertainties related to detector performance do not cancel in R_{dA} , because the two data sets were taken under different running conditions. The global scaling uncertainty in $\langle N_{\text{coll}} \rangle$ and the BBC efficiency is shown as a box centered around unity at the right edge of the plot.

For the most peripheral collisions in both rapidity ranges, R_{dA} shows no overall modification. For the most central collisions, a clear enhancement is observed at backward rapidity. This enhancement suggests nuclear- p_T broadening at moderate p_T , which is similar to that seen at midrapidity [17], and gluon antishadowing. In the 0%-20%

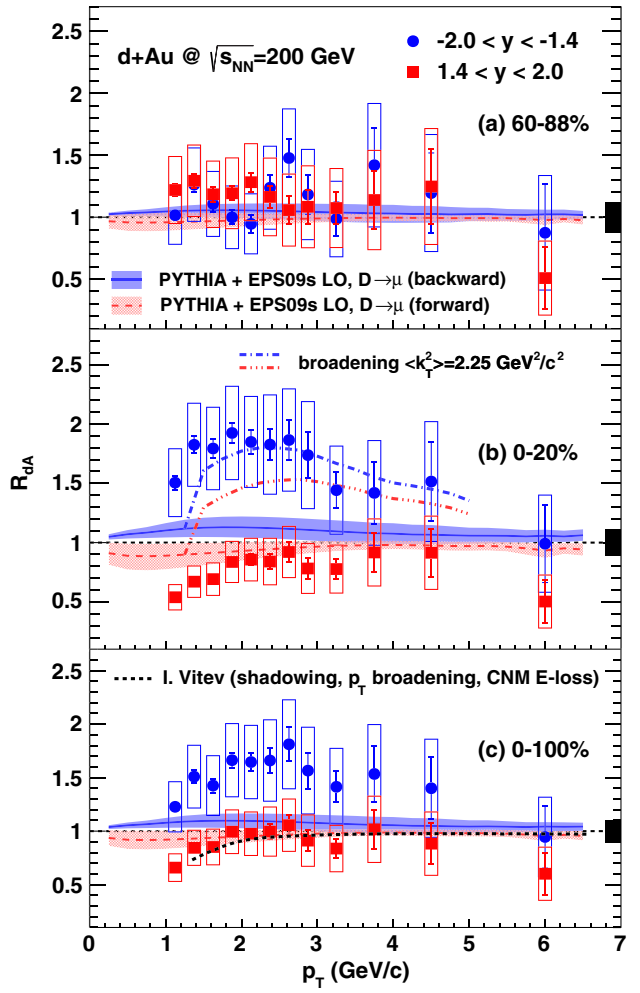


FIG. 2 (color online). The nuclear modification factor R_{dA} for negatively charged heavy-flavor muons in $d + \text{Au}$ collisions for the (a) most peripheral (60%-88%) and (b) most central (0%-20%) centrality classes, and (c) unbiased (0%-100%) data. The black boxes on the right side indicate the global scaling uncertainty. The red dashed (blue solid) lines in each panel are calculations at forward (backward) rapidity based on the EPS09s nPDF set [14]. Dot-dashed curves in (b) are the same calculations plus an additional nuclear- p_T broadening. The theoretical calculation shown in (c) is for forward rapidity [16].

of most central collisions, the forward rapidity R_{dA} shows a global suppression, presumably caused by gluon shadowing and/or partonic energy loss, which becomes stronger at low p_T and is probably a sign of nuclear- p_T broadening.

The dotted line in Fig. 2(c) is a prediction of R_{dA} for muons from D and B mesons at forward rapidity, $y = 1.7$ [16,27]. This prediction, including CNM effects such as shadowing, initial-state energy loss, and nuclear- p_T broadening, is consistent with the data at forward rapidity for the 0%-100% centrality class. The same model, with additional energy loss in deconfined hot nuclear matter, also describes the forward heavy-flavor muon results in central Cu + Cu collisions within uncertainties [8]. This

agreement and the suppression at forward rapidity in central $d + \text{Au}$ collisions suggest that CNM effects are important for the interpretation of the suppression of heavy-flavor muon production at forward rapidity at RHIC [8] and the Large Hadron Collider [28].

We use the EPS09s leading-order (LO) nuclear PDF (nPDF) set [14] to calculate R_{dA} for muons from D mesons at backward (solid lines) and forward (dashed lines) rapidity based solely on initial parton density modifications. As described in [29], the input parameters for the EPS09s calculation [14], which incorporates a spatial dependence within the nucleus based on the previous nPDF EPS09 model [13], are the parton momentum fraction x , momentum transfer (Q^2) of charm production generated by PYTHIA [15], and transverse radial positions of binary collisions in the nucleus for each centrality class. The uncertainty bands are calculated as described in [13].

In central collisions, shown in Fig. 2(b), the EPS09s-nPDF-based calculation does not reproduce the data at backward rapidity (Au-going direction), particularly in the moderate p_T region. At forward rapidity (d -going direction), R_{dA} calculated with the EPS09s nPDF is consistent with the data over the entire p_T range within the uncertainties of the data and calculation. The same EPS09s-nPDF-based calculations with a nuclear-multiple-scattering broadening $\langle k_T^2 \rangle = 2.25 \text{ GeV}^2/c^2$ (dot-dashed lines), when selected to match the backward rapidity data, overshoot the data at forward rapidity. There is no consistent combination of nuclear- p_T broadening and modified nPDF that can describe the entire rapidity dependence of the data. A model incorporating scattering and recombination with soft and hard final-state gluons [30] explains the enhancement of hadrons at the higher-parton-density backward rapidity and no enhancement at the lower-parton-density forward rapidity [30], noting the larger particle production resulting from higher parton density [31,32]. It would be interesting to see if this model, once extended to charm hadrons, accommodates the entire rapidity of the data presented here.

Figure 3 shows the heavy-flavor muon and electron [17] R_{dA} as a function of $\langle N_{\text{coll}} \rangle$ for (a) $1 < p_T < 3 \text{ GeV}/c$ and (b) $3 < p_T < 5 \text{ GeV}/c$. Bars (boxes) around the data points represent the statistical (total) uncertainties determined as the quadratic sum of statistical (total) uncertainties on R_{dA} for each centrality class. The global uncertainty reflects the BBC efficiency for $p + p$ collisions. For more central $d + \text{Au}$ collisions, the R_{dA} at midrapidity and backward rapidity show a similar enhancement ($R_{dA} > 1$) in both p_T ranges. The low-and high- p_T bins show comparable suppression patterns as a function of centrality. The EPS09s-nPDF-based calculations are qualitatively consistent with the data.

Quarkonia and open heavy-flavor hadrons are sensitive to the same effects on heavy-quark production. However, quarkonium states are additionally influenced by breakup

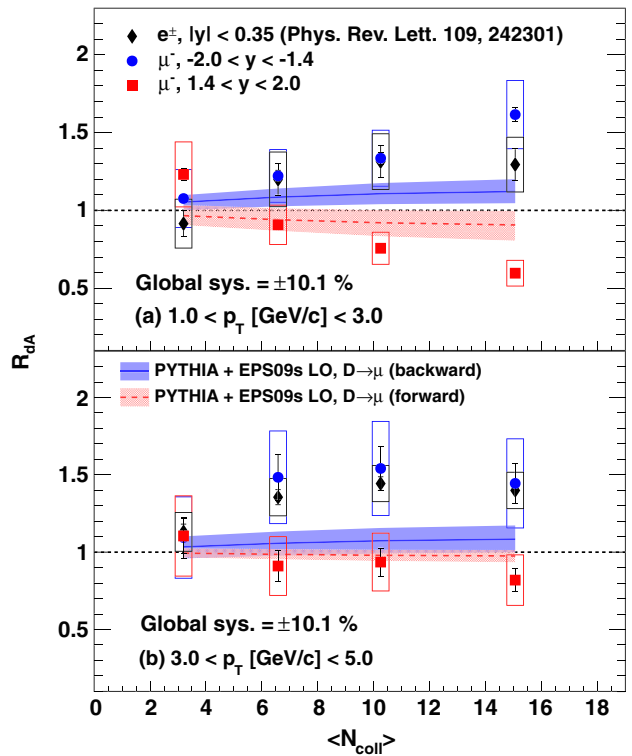


FIG. 3 (color online). Comparison of R_{dA} as a function of $\langle N_{\text{coll}} \rangle$ for heavy-flavor leptons from different rapidity and p_T bins. Data in the top (bottom) panel are from low ($1 < p_T < 3 \text{ GeV}/c$) and moderate ($3 < p_T < 5 \text{ GeV}/c$) p_T ranges. Diamonds represent heavy-flavor electrons at midrapidity [17] and squares (circles) represent heavy-flavor muons at forward (backward) rapidity.

in nuclear matter. Therefore, open heavy-flavor production can provide a baseline for interpreting the nuclear breakup of quarkonia. Previous measurements suggest that nuclear breakup has a significant effect on quarkonium production in p -nucleus and nucleus-nucleus collisions [21,29,33–37].

Figure 4 shows a comparison of R_{dA} between heavy-flavor muons and J/ψ [21] for central collisions. A similar behavior across the entire p_T range is observed at forward rapidity, within the total uncertainties, whereas a distinct difference is seen at backward rapidity, particularly for $p_T < 2.5 \text{ GeV}/c$, where charm contributions dominate over those from the bottom [38]. The larger difference of the R_{dA} between J/ψ and open charm at backward rapidity compared to forward rapidity could be related to the longer time this $c\bar{c}$ state requires to traverse the nuclear matter or the larger density of comoving particles after the initial collision at backward rapidity [39]. This comparison suggests that an additional CNM effect, nuclear breakup, significantly affects J/ψ production both at backward rapidity and, as seen earlier [17,21], at midrapidity. This measurement provides a key additional constraint on theoretical models attempting to describe quarkonia yields in nuclear collisions.

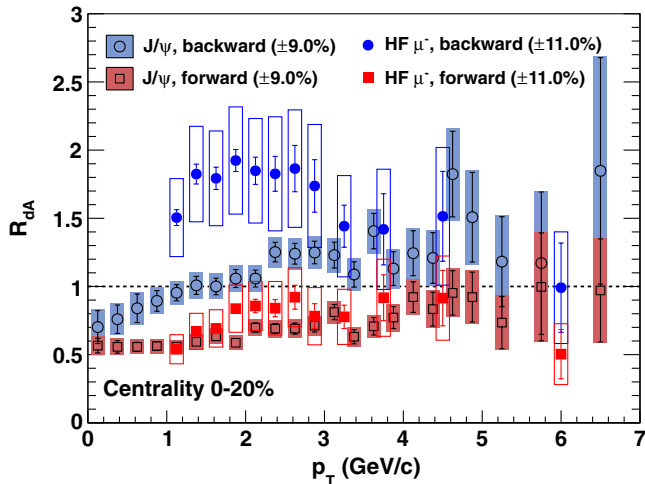


FIG. 4 (color online). The nuclear modification factor R_{dA} for J/ψ [21] and heavy-flavor muons for the 0%–20% centrality class. The global systematic uncertainty on each distribution is shown as a percentage in the legend.

We have presented a measurement of negatively charged heavy-flavor muons produced at forward and backward rapidity in $d + \text{Au}$ collisions at $\sqrt{s_{NN}} = 200$ GeV, for several centrality classes. We observe no significant modification in the most peripheral $d + \text{Au}$ collisions. However, in central $d + \text{Au}$ collisions, suppression (enhancement) of heavy-flavor muons is observed at forward (backward) rapidity. The large difference between forward and backward rapidity, which cannot be reproduced by PYTHIA calculations with the EPS09s nPDF sets nor with the combination of additional nuclear- p_T broadening, suggests the importance of CNM effects beyond nPDF modification, as well as the possibility of final-state interaction in $d + \text{Au}$ collisions. A model including some of these effects successfully reproduces an enhanced hadron production in a higher-parton-density system. A comparison between the measured nuclear modification factors for J/ψ and open heavy-flavor production provides a strong indication that nuclear breakup significantly affects quarkonium production.

We thank the staff of the Collider-Accelerator and Physics Departments at Brookhaven National Laboratory and the staff of the other PHENIX participating institutions for their vital contributions. We acknowledge support from the Office of Nuclear Physics in the Office of Science of the Department of Energy, the National Science Foundation, Abilene Christian University Research Council, Research Foundation of SUNY, and Dean of the College of Arts and Sciences, Vanderbilt University (U.S.A), Ministry of Education, Culture, Sports, Science, and Technology and the Japan Society for the Promotion of Science (Japan), Conselho Nacional de Desenvolvimento Científico e Tecnológico and Fundação de Amparo à Pesquisa do Estado de São Paulo (Brazil), Natural Science Foundation

of China (P. R. China), Ministry of Education, Youth and Sports (Czech Republic), Centre National de la Recherche Scientifique, Commissariat à l’Énergie Atomique, and Institut National de Physique Nucléaire et de Physique des Particules (France), Bundesministerium für Bildung und Forschung, Deutscher Akademischer Austausch Dienst, and Alexander von Humboldt Stiftung (Germany), Hungarian National Science Fund, OTKA (Hungary), Department of Atomic Energy and Department of Science and Technology (India), Israel Science Foundation (Israel), National Research Foundation and WCU program of the Ministry Education Science and Technology (Korea), Physics Department, Lahore University of Management Sciences (Pakistan), Ministry of Education and Science, Russian Academy of Sciences, Federal Agency of Atomic Energy (Russia), VR and Wallenberg Foundation (Sweden), the U.S. Civilian Research and Development Foundation for the Independent States of the Former Soviet Union, the Hungarian American Enterprise Scholarship Fund, the US-Hungarian Fulbright Foundation for Educational Exchange, and the US-Israel Binational Science Foundation.

^{*}Deceased.

[†]PHENIX Co-Spokesperson.

morrison@bnl.gov

[‡]PHENIX Co-Spokesperson.

jamie.nagle@colorado.edu

- [1] B. Abelev *et al.* (ALICE Collaboration), *J. High Energy Phys.* **09** (2012) 112.
- [2] B. Abelev *et al.* (ALICE Collaboration), *Phys. Rev. Lett.* **111**, 102301 (2013).
- [3] S. S. Adler *et al.* (PHENIX Collaboration), *Phys. Rev. D* **76**, 092002 (2007).
- [4] A. Adare *et al.* (PHENIX Collaboration), *Phys. Rev. Lett.* **97**, 252002 (2006).
- [5] H. Agakishiev *et al.* (STAR Collaboration), *Phys. Rev. D* **83**, 052006 (2011).
- [6] S. S. Adler *et al.* (PHENIX Collaboration), *Phys. Rev. Lett.* **96**, 032301 (2006).
- [7] A. Adare *et al.* (PHENIX Collaboration), *Phys. Rev. Lett.* **98**, 172301 (2007).
- [8] A. Adare *et al.* (PHENIX Collaboration), *Phys. Rev. C* **86**, 024909 (2012).
- [9] M. G. Mustafa, *Phys. Rev. C* **72**, 014905 (2005).
- [10] G. D. Moore and D. Teaney, *Phys. Rev. C* **71**, 064904 (2005).
- [11] H. van Hees, V. Greco, and R. Rapp, *Phys. Rev. C* **73**, 034913 (2006).
- [12] M. Djordjevic, *Phys. Rev. C* **74**, 064907 (2006).
- [13] K. J. Eskola, H. Paukkunen, and C. A. Salgado, *J. High Energy Phys.* **04** (2009) 065.
- [14] I. Helenius, K. J. Eskola, H. Honkanen, and C. A. Salgado, *J. High Energy Phys.* **07** (2012) 073.
- [15] T. Sjostrand, S. Mrenna, and P. Z. Skands, *J. High Energy Phys.* **05** (2006) 026; PYTHIA, version 6.421 with modified parameters, pmass(4,1)=1.25 (m_c), parp(31)=1 (K factor),

- mstp(32) = 4 ($Q^2 = \hat{s}$), mstp(33) = 1, parp(91) = 0 and 1.5 ($\langle k_T \rangle$).
- [16] I. Vitev, *Phys. Rev. C* **75**, 064906 (2007).
- [17] A. Adare *et al.* (PHENIX Collaboration), *Phys. Rev. Lett.* **109**, 242301 (2012).
- [18] M. Allen *et al.* (PHENIX Collaboration), *Nucl. Instrum. Methods Phys. Res., Sect. A* **499**, 549 (2003).
- [19] S. N. White, *AIP Conf. Proc.* **792**, 527 (2005).
- [20] M. L. Miller, K. Reygers, S. J. Sanders, and P. Steinberg, *Annu. Rev. Nucl. Part. Sci.* **57**, 205 (2007).
- [21] A. Adare *et al.* (PHENIX Collaboration), *Phys. Rev. C* **87**, 034904 (2013).
- [22] A. Adare *et al.* (PHENIX Collaboration), *Phys. Rev. C* **88**, 024906 (2013).
- [23] K. Adcox *et al.* (PHENIX Collaboration), *Nucl. Instrum. Methods Phys. Res., Sect. A* **499**, 469 (2003).
- [24] H. Akikawa *et al.* (PHENIX Collaboration), *Nucl. Instrum. Methods Phys. Res., Sect. A* **499**, 537 (2003).
- [25] A. Adare *et al.* (PHENIX Collaboration), *Phys. Rev. C* **84**, 044905 (2011).
- [26] J. K. Yoh *et al.*, *Phys. Rev. Lett.* **41**, 684 (1978).
- [27] R. Sharma, I. Vitev, and B.-W. Zhang, *Phys. Rev. C* **80**, 054902 (2009).
- [28] B. Abelev *et al.* (ALICE Collaboration), *Phys. Rev. Lett.* **109**, 112301 (2012).
- [29] J. L. Nagle, A. D. Frawley, L. A. Linden Levy, and M. G. Wysocki, *Phys. Rev. C* **84**, 044911 (2011).
- [30] R. C. Hwa and C. B. Yang, *Phys. Rev. Lett.* **93**, 082302 (2004).
- [31] B. Back *et al.* (PHOBOS Collaboration), *Phys. Rev. Lett.* **93**, 082301 (2004).
- [32] I. Arsene *et al.* (BRAHMS Collaboration), *Phys. Rev. Lett.* **94**, 032301 (2005).
- [33] A. Adare *et al.* (PHENIX Collaboration), *Phys. Rev. C* **77**, 024912 (2008).
- [34] A. Adare *et al.* (PHENIX Collaboration), *Phys. Rev. Lett.* **111**, 202301 (2013).
- [35] A. Adare *et al.* (PHENIX Collaboration), *Phys. Rev. Lett.* **107**, 142301 (2011).
- [36] B. Z. Kopeliovich, I. K. Potashnikova, and I. Schmidt, *Nucl. Phys.* **A864**, 203 (2011).
- [37] C. Lourenco, R. Vogt, and H. K. Woehri, *J. High Energy Phys.* **02** (2009) 014.
- [38] A. Adare *et al.* (PHENIX Collaboration), *Phys. Rev. Lett.* **103**, 082002 (2009).
- [39] R. Vogt, *Phys. Rev. C* **61**, 035203 (2000).